Localized Excitations and Anisotropic Directional Ordering in a Two-Dimensional Morse Lattice Model of Cuprate Layers

Manuel G. Velarde, Werner Ebeling, and Alexander P. Chetverikov

Abstract We study here localized excitations in a Morse lattice model of two-dimensional CuO_2 layers (cuprates in short). The Cu-atoms are positioned motionless in a square lattice and the oxygen atoms are able to oscillate around originally equilibrium positions on another superposed square lattice. After studying regular oxygen lattices we investigate lattices with bonds which are weakly distorted. We estimate the density of compressions (strain density) in dependence of the misfit of the Cu–O-bonds. We show that with increasing misfit the nonlinear oscillations of the O-atoms yield stripes hence patches exhibiting anisotropic directional ordering with an overall yet transient tessellated structure.

1 Introduction

The model system which we study here is a square lattice with lattice constant σ (equilibrium distance between lattice units), formed by oxygen atoms, which is embedded or superposed into another square lattice, consisting of copper atoms.

M.G. Velarde (✉)
Instituto Pluridisciplinar, Universidad Complutense, Paseo Juan XXIII, 1, Madrid-28040, Spain

Fundación Universidad Alfonso X El Sabio, Villanueva de la Cañada-28691, Madrid, Spain
e-mail: mgvelarde@uax.es,mgvelarde@pluri.ucm.es

W. Ebeling
Instituto Pluridisciplinar, Universidad Complutense, Paseo Juan XXIII, 1, Madrid-28040, Spain

Institut für Physik, Humboldt-Universität Berlin, Newtonstrasse 15, Berlin-12489, Germany
e-mail: ebeling@physik.hu-berlin.de

A.P. Chetverikov
Instituto Pluridisciplinar, Universidad Complutense, Paseo Juan XXIII, 1, Madrid-28040, Spain

Department of Physics, Saratov State University, Astrakhanskaya 83, Saratov-410012, Russia
e-mail: chetverikovap@info.sgu.ru

R. Carretero-González et al. (eds.), *Localized Excitations in Nonlinear Complex Systems*, Nonlinear Systems and Complexity 7, DOI 10.1007/978-3-319-02057-0_10,

© Springer International Publishing Switzerland 2014

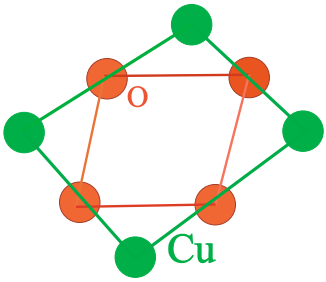


Fig. 1 Model CuO_2 cuprate layer. Two superposed square lattices, one with oxygens (*red color dots*) and another with coppers (*green color dots*)

We assume that the interaction potential parameters are such that the distances between minima of *Cu* and of *O* – atoms are related like the geometrical distances as $1/\sqrt{2}$ [1, 2]. This case is denoted as "regular"; otherwise, if the distances deviate from such value we speak about "irregular" cases. The case of a regular lattice exhibiting breathers was already considered by Russell and colleagues [3–5]. For other works on breathers for two-dimensional lattices see Refs. [6–11]. Here we shall explore stripe structures and soliton-like localized excitations rather than breathers. In the case of heated lattices, irregular configurations may appear as time proceeds, so the term regular and irregular refers only to the initial *equilibrium* situation. Note that we give only the initial square lattice configuration and then we allow the *O*-units to freely move, but the *Cu*-units are held fixed in the time scale considered here which agrees with available experimental observations [12, 13].

Figure 1 provides a schematic representation of our model two-lattice problem. The motivation of our study comes from arguments proposed by Müller [12, 13], Busmann-Holder [14–16], Newns and Tsuei [17, 18] and Alexandrov [19] and the need of interpreting experimentally observed facts. Long ago Müller [12] when discussing significant features of high-Tc superconductors (HTSC) underlined the possible role of anharmonic phonons. He proposed a model of anharmonic vibrations of apical oxygens interacting with carriers in CuO_2 planes. Recent topographic and other studies give us a lot of detailed information about the microscopic charge distributions [20–26]. Typically "stripe" patterns are observed whose structure depends on charge doping. Accordingly, we assume that below the HTSC regime exists a regime of stripes (electronic glass). Here we show that the long range uniform order may be broken leading to a kind of dynamic tessellation patterns.

In particular we consider here a model for multistable lattices first introduced by Bussmann-Holder [14–16] and similar to the fluctuating bonds model proposed by Newns and Tsuei [17,18]. In this, our first approach to the above posed experimental evidence, no excess added electrons are considered here as our aim is not the study of the superconducting regime itself, but merely to analyze the role and influence of lattice nonlinearities leading to localized excitations and anisotropic directional ordering along certain axes of the cuprate lattice layer.

We start with the case of nonlinear oscillations of cuprate planar lattices with regular structure (see also [3–5]). Then we include qualitatively the expected effect

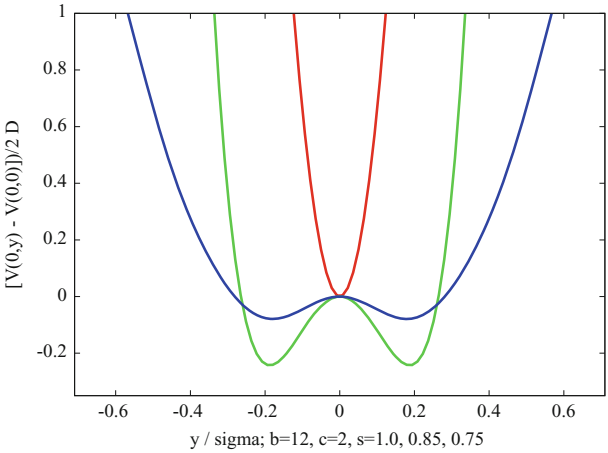


Fig. 2 Possibilities (minima) offered to an oxygen atom by a quartic potential (1). The single minimum curve corresponds to no doping. As charge doping enters we have two symmetric stable equilibria. The abcissa axis is orthogonal to the *Cu–Cu* line with units are proportional to the *O–O* distance divided by σ

of some weak doping by assuming that the bond length *Cu–O* is increased due to added, excess free charges. Following Newns and Tsuei [17, 18] the charges lead to instability of the originally equilibrium regular *O*-positions between two copper atoms which are replaced by two new, equally available, stable positions. This is locally accounted by a fourth-order nonlinearity in the energy,

$$E_O \simeq E_0 - g_2 y^2 + g_4 y^4, \tag{1}$$

where y is a coordinate perpendicular to the direct connection between two copper atoms and $g_i (i = 2, 4)$ are parameters of the potential. Then depending on the sign of g_2 the double-well quartic potential could accommodate bistable oxygen configurations (Fig. 2). However we will not use (1) but rather a Morse potential locally exhibiting the same feature. The Morse interatomic potential is the first quantum based one. It does not differ significantly from the (12,6) Lennard-Jones potential of much current use [2, 27, 28]. It differs from the Toda potential [29] only in the attractive component which is unphysical in the Toda case. The Toda dynamic problem is exactly solvable in the one-dimensional (1d) case, and it is known that differences in the actual form of its solutions relative to the numerical solutions of the Morse dynamic problem are within 10 % deviation [30, 31]. Accordingly, we shall use the explicitly known analytical solutions of the Toda lattice to guide us in the computer simulations with the Morse potential.

Let us emphasize that the energy landscape (1) proposed by Newns and Tsuei [17, 18] comes from an ab initio quantum mechanical calculation for small lattice displacements. Yet in order to allow free oxygen motions, as stated above, we

need an interaction potential which, for our molecular dynamics computational algorithm, has free asymptotics at large inter-unit distances. This is possible with the Morse or the Lennard-Jones potential. However, we prefer the former since it corresponds better to quantum-mechanical repulsion at short inter-unit distances, which is the region of significance in our approach here. The quantum mechanical calculations made by Newns, Tsuei and collaborators [18] use "frozen" configurations to obtain (1). Locally, our Morse potential is chosen to fit their data thus ensuring the correct polynomial expansion around the potential minimum while being more physically acceptable at quite short (and also long) inter unit distances.

For simplicity we have placed all *Cu*-atoms and *O*-atoms superposed into a single and same plane (Fig. 1). This is not completely realistic, so our *O*- and *Cu*-atoms are a kind of suitable projections of the real atoms. The players in our nonlinear dynamics are the *O*-atoms which are oscillating atoms interacting with six neighbors (in the initial configuration). Four of the neighbors are also *O*-atoms and the two other are *Cu*-atoms which as earlier noted will be motionless. The *Cu*-sub-lattice gives the frame for our game, the *O*-atoms are quite free and are looking for the "best place" according to the Morse interactions which locally correspond also to the double-well quartic potential (1).

2 Model Hamiltonian and Visualization of Local and Collective Atom (Lattice Units) Motions

We write the lattice Hamiltonian as

$$H_a = \sum_n \frac{m}{2} v_n^2 + \frac{1}{2} \sum_{n,k'} V^M_{Cu-O} \left(|r_n - r_{k'}|\right) + \frac{1}{2} \sum_{n,j} V^M_{O-O} \left(\left|r_n - r_j\right|\right), \quad (2)$$

where the subscripts locate atoms sitting near to lattice sites and for the summations over n and j run from 1 to N_O while the summations over k' from 1 to N_{Cu} with subscripts O and Cu referring to oxygen and copper, respectively (N denotes number of units). All masses are taken equal: $m_n = m$ for all n. The Morse potential we use is

$$V^M(r) = D\left[\exp(-2b(r-\sigma)) - 2\exp(-b(r-\sigma))\right], \quad (3)$$

where D, b, σ denote the corresponding potential-well depth, lattice stiffnesses and initial inter unit equilibrium distances (D_{O-O}, b_{O-O}, σ_{O-O} for oxygen-oxygen interactions, and D_{O-Cu}, b_{O-Cu}, σ_{O-Cu} for oxygen-copper interactions). The free space variable r will be subsequently considered in the two dimensional (x, y) plane with complex coordinates, and hence r would be replaced by $Z = x + iy$.

Putting the *Cu*-atoms and *O*-atoms together and giving full freedom to the *O*-atoms, as time proceeds we are bound to obtain a complex multi-stable potential landscape. In order to observe the rather complex dynamics in such "regular" or

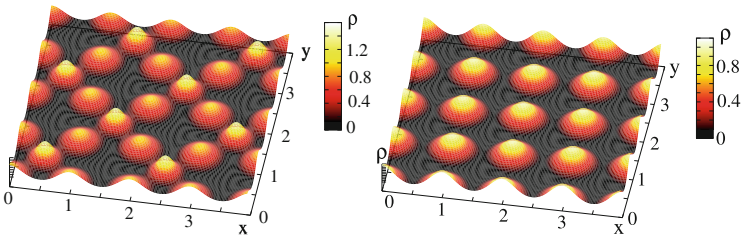


Fig. 3 *Left panel*: Visualization of copper atoms (narrower peaks) and oxygen atoms (broader peaks) (compound of both terms in Eq. (4)) by considering that atoms may be described as Gaussian densities of their core electrons in a regular lattice with bond lengths in the $\sqrt{2}$ ratio as required by the regular geometry at zero T ($\eta = 1/\sqrt{2}$; $\lambda_O = 0.25$, $\lambda_{Cu} = 0.177$, $T = 0.0002 D_{O-O}$). *Right panel* shows only the oxygen units (first term in Eq. (4))

"irregular" lattices we need an appropriate method of visualization. We model the lattice units or atoms as points on a plane which are surrounded by little spheres formed by the atomic electrons. We will assume that these atomic electrons may be represented by a Gaussian distribution centered on each lattice site. Accordingly, in Fig. 3 the left panel indicates how to experimentally observe atom motions and eventually moving local excitations by means of, e.g., Scanning Tunneling Microscopy (STM) or a more appropriately faster scanning methodology [32]. When two atoms approach each other like in a strong enough compression the superposition of their corresponding electron Gaussian densities yield, e.g., an enhanced single maximum out of the composition of the original two separated maxima. For a thorough discussion of this methodology and earlier results in lattice systems the reader is referred to [33–38]. The compound electron density is then:

$$\rho(Z,t) = \sum\nolimits_{n;|Z-Z_n(t)|<1.5} \exp\left[-\frac{|Z-Z_n(t)|^2}{2\lambda_O^2}\right], \\ \sum\nolimits_{k',|Z-Z_{k'}|<1.5} \exp\left[-\frac{|Z-Z_{k'}|^2}{2\lambda_{Cu}^2}\right]. \tag{4}$$

Here the Z_n are the complex oxygen coordinates, rescaled using as unit σ_{O-O}. We will use different λ-parameters for oxygen and for copper, (λ_O and λ_{Cu}, respectively) taking into account their different atom size. Note in Fig. 3 that copper-peaks are narrower than oxygen peaks. Needless to say when only oxygens are displayed there is no contribution from the second term in the r.h.s. of (4).

We denote by σ_{O-O} and σ_{O-Cu} the actual distances between two oxygen units and between an oxygen unit and a copper unit in the regular geometrical configuration. Then we define $\eta \equiv \sigma_{O-Cu}/\sigma_{O-O}$. Note that σ_{Cu-Cu} is of no relevance as it remains with a fixed constant and the same value at all times. Besides σ_{O-O} is the reference value and, consequently, only σ_{O-Cu} relative to σ_{O-O} is allowed to change.

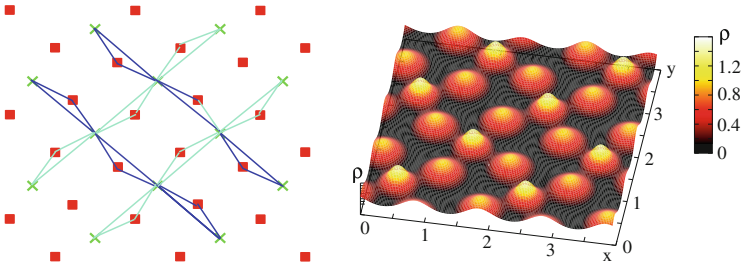


Fig. 4 Two-lattice model cuprate layer. *Left panel*: CuO_2 lattice illustrating one among the two possible oxygen configurations for η slightly different from $1/\sqrt{2}$ (see also the single minimum in Fig. 2). *Right panel*: Snapshot of an equivalent visualization of *left panel* for $\eta = 0.74$ in a rather cold lattice ($T = 2.10^{-4} D_{O-O}$). Enhanced (narrower) peaks correspond to copper units. Parameter values: $(b\sigma)_{O-O} = (b\sigma)_{O-Cu} = 10$, $D_{O-Cu}/D_{O-O} = 1.5$, $\lambda_O = 0.2$, $\lambda_{Cu} = \lambda_O \eta$

From the Hamiltonian (2) with (3) we can get the corresponding Newton's equations of motions. However, as we want to play with temperature we introduce heating by introducing in the dynamic system an appropriate thermal bath. Hence the evolution of the oxygen atoms is governed by the Langevin equations:

$$d^2 Z_n/dt^2 = \sum\nolimits_k F_{nk}^{O-O}\left(|Z_{nk}|\right) z_{nk} + \sum\nolimits_{k'} F_{nk'}^{O-Cu}\left(|Z_{nk'}|\right) z_{nk'}$$
$$- \gamma dZ_n/dt + \sqrt{2D_v}\left(\xi_{nx} + i\xi_{ny}\right), \tag{5}$$

where now, for better clarity, n and k denote lattice positions of the oxygens and k' those of coppers; $Z_{nk} = Z_n - Z_k$ and $z_{nk} = Z_{nk}/|Z_{nk}|$. γ, D_v and ξ_s account for friction, noise strength and noise fluctuating variables. Temperature is thus defined using Einstein's relation $T = D_v/\gamma$ (in computations we use $\gamma = 0.2$ or 0.02).

The forces are

$$F_{nk}^{O-O}\left(|Z_{nk}|\right) = -dV_{O-O}^{M}(r)/\,dr|_{r=|Z_{nk}|}\,, \tag{6}$$

and

$$F_{nk'}^{O-Cu} = -dV_{O-Cu}^{M}(r)/\,dr|_{r=|Z_{nk'}|}\,. \tag{7}$$

The quantity V^M accounts for both terms in (2). All computer simulations start with a lattice equilibrium distribution. Then after integrating Eq. (5) we wait for a *steady state* corresponding to the a priori fixed temperature.

Figure 4 shows the *Cu*-atoms as enhanced peaks in a landscape of *O*-densities (right panel). With these assumptions we study the oxygen dynamics seeing the fixed copper positions only in enlarged zoomed pictures. For simplicity and illustration of results we set $\lambda_{Cu} \equiv \lambda_O \eta$ with parameter λ to be allowed to vary at will. Note that we use σ_{O-O} and $2D_{O-O}$ as distance and energy units, respectively.

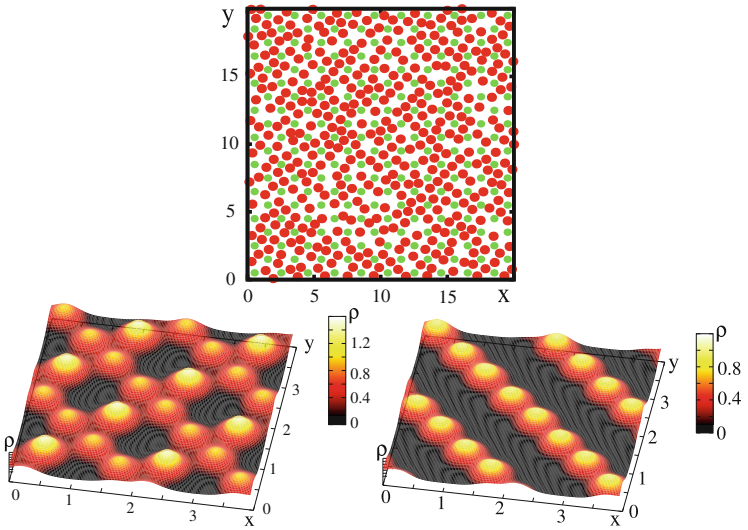


Fig. 5 Snapshots of a cuprate layer slightly heated. *Upper panel*: Snapshot of the cuprate layer with irregular bonds. Most of the oxygen units (*red dots*) are off their original equilibrium centers of the connecting lines between the copper units (see Fig. 1). *Left panel below*: Snapshot of an enlarged view of a portion of the *upper panel*. Such a portion shows one among many other patches where we see in the patch rather long range anisotropic liquid-crystalline directional ordering as further illustrated in the *lower right panel*, where, extracted from the *lower left panel*, only the oxygen atoms are displayed. Parameter values and temperature as in Fig. 4, save $\eta = 0.95$

Besides $(b\sigma)_{O-O} = (b\sigma)_{O-Cu} = 5$ or 10 in our computations. In order to represent the bonds between Cu–O and their evolution we play with the free lambda-parameter looking for values which allow an easy representation of bond structure.

Note that as oxygen motions get stronger and stronger the apparent symmetry shown in the Fig. 4 will be altered with the possibility of configurations with many more oxygen units aligned together albeit always within patches, as displayed in Fig. 5.

Two cases are of interest:

(i) **Case 1**: In the absence of added, excess free electrons (no doping), the O-atoms are sitting in equilibrium on a square lattice where they are located halfway between the Cu-atoms. When heating the system the O-atoms perform nonlinear oscillations. In an ideal regular lattice $\eta = 1/\sqrt{2}$; the effective binding radii are in $\sqrt{2}$ ratio as indicated in the Introduction. According to Pauling [1,2] the actual ratio between lattice radii is around $0.96/1.40 \simeq 0.69$ which is near to $1/\sqrt{2} = 0.707$.

(ii) **Case 2**: At stronger but still undercritical doping we have according to the fluctuating bond effect [17,18] a small increase of the bond length $\eta(n) > 1/\sqrt{2}$ where the parameter n denotes doping percentage due to the added, excess free electrons. This is expected to lead to the formation of "stripes" which we are going to study in the following section.

3 Simulation of the Oxygen Dynamics

We start with some computer simulations of the regular or nearly regular case. According to Newns and Tsuei [17, 18], a finite amount of doping changes the effective binding length $Cu - O$ and eventually leads to bistable configurations. For a qualitative (mean field) account of this effect we assume that the length ratio, η, increases nearly linearily with the doping percentage, n, and hence

$$\eta(n) = 1/\sqrt{2} + \alpha n + \ldots,$$

where n is assumed weak. Let us further assume that $(b\sigma)_{O-O} = 5$ or 10 is the stiffness of the $O - O$ potential and $(b\sigma)_{O-Cu}$ the stiffness of the $Cu - O$ potential which is assumed to have the same value as the former.

We investigate now the energy landscape of a system admitting some small misfit of the parameter values and show that this may lead indeed to fluctuating bonds. We remind that we take the equilibrium distance between two O-atoms σ_{O-O} as the unit of length. Furthermore in our model the equilibrium distance of $Cu - O$ is $\sqrt{2}\sigma_{O-O}/2$ and the $Cu - Cu$ equilibrium distance is $\sigma_{O-O}\sqrt{2}$.

Let us analyze the consequences of small changes of the bond length. We expect that an increased bond length $Cu - O$ will push the oxygens off the initial axes and will create a positive or negative elongation (Fig. 4, left panel). Recall that we consider one O-atom initially in a "cage" surrounded by four O-atoms and 2 Cu-atoms. The potential in the center of the cage may be represented by 6 contributions from the 6 neighbors and shows bistability indeed for appropriate parameter values.

The "fluctuating bond" condition is that the extremum connected with the regular position is higher than the global minimum what means in effect that the regular position is unstable. The condition that the side minima are deeper than the central extremum may be fulfilled for a large set of parameter values. The search for an appropriate set is quite complicated. Various cases are illustrated in Figs. 5 and 6.

4 Discussion and Conclusions

We have studied here the localized excitations in a Morse model of regular and irregular CuO_2 (cuprate) lattices under different conditions. Irregular lattices are obtained by introducing some small misfit of bond lengths. In the framework of the Newns-Tsuei fluctuating bond model [17, 18] this may be interpreted as due to electron doping in the cuprate layer i.e. due to adding excess free electrons, but a discussion of this latter point is beyond the scope of our interest here.

Consequently, the anharmonic oxygen motions, originally suggested by Müller [12] appear as a possible explanation for the observed stripe structures in cuprates [20–26]. We assumed here that such changes due to doping have the physical meaning that the ratio of the length of the $Cu - O$ bond to the $O - O$ bond may vary.

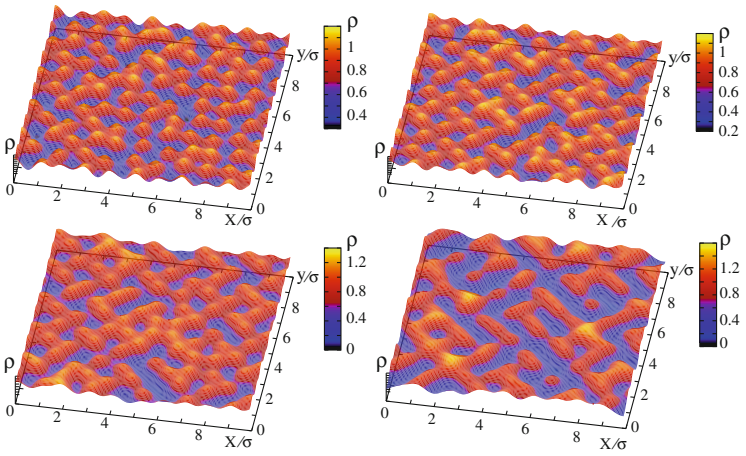


Fig. 6 Snapshots of a cuprate layer at a higher temperature than in Fig. 5. *Upper left panel*: $\eta = 0.74$; *upper right panel*: $\eta = 0.80$; *lower left panel*: $\eta = 0.85$; and *lower right panel*: $\eta = 0.95$. Note the difference between the latter case with the case of Fig. 5 for $\eta = 0.95$. For purpose of easier visualization only the oxygen densities are provided as also done in the *right panel* of Figs. 3 and 5. Note that the long range anisotropic directional order is eventually weakened as temperature grows. Parameter values: $(b\sigma)_{O-O} = (b\sigma)_{O-Cu} = 5$, $D_{O-Cu}/D_{O-O} = 1$, $\lambda_O = 0.35$, $T = 0.2D_{O-O}$ and $\gamma = 0.02$

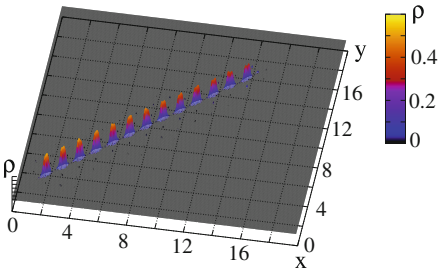


Fig. 7 Cumulative picture of a sequence of snapshots (all plotted in the same picture) to illustrate the trajectory of a soliton-like localized compression density in a lattice of oxygen atoms in a regular cuprate lattice launched by a strong pulse (momentum given) to one O-atom in the direction of the already ordered O-line. Parameter values: $\eta = 1/\sqrt{2}$, $\lambda_O = 0.25$, and all other parameters have the same values as in Fig. 6

In order to check this idea we played with the bond length of the original system where this ratio is approximately given by $1/\sqrt{2}$. The result is that the changes of the bond length are correlated with the nonlinear oxygen oscillations in the lattice and the multistability of configurations.

What can we say about solitonic excitations? From our present knowledge we can say that we can successfully launch solitons as shown in Fig. 7 by, e.g., giving momentum (giving a sudden kick) to one oxygen atom in a row of rectilinearly

arranged O-atoms in the direction of the row thus benefiting from the rather long range anisotropic liquid crystalline-like directional ordering observed in one many patches in the lattice. Those patches may join with the possible consequence of creating a "percolation" transport path as the density of "patches" with such ordering is increased. Already "static" percolation via "plaquettes" of ordering has been suggested recently albeit with no electron-phonon interaction [39]. Here however we offer a possible dynamic percolation. Solitonic pulses can then propagate along the oxygen lines. Such rectilinear oxygen lines we can identify in regular lattices. In the rectilinear rows of oxygen, oriented along $Cu - Cu$ axes, in Figs. 3 or 4 the oxygen distances are too large, in average $\sqrt{2}\sigma_{O-O}$. Nevertheless we were able to excite solitons by very strong initial pulses. In the case of irregular bonds as illustrated in Fig. 5 we see the formation of rectilinear oxygen rows with rather small interatomic distances. This way we can foresee a much easier excitation of solitons along the rows.

Our basic parameter is the ratio of the radii $\eta = \sigma_{O-Cu}/\sigma_{O-O}$. For a regular lattice the ideal ratio is $1/\sqrt{2}$. For higher values of this ratio (irregular lattices) we observe bistability and the potential reminds then the quartic type potential along the axis perpendicular to the $Cu - Cu$-bond calculated by Newns and Tsuei [17,18].

The Cu-lattice gives the static frame for our computer runs and the O-atoms are quite free and are looking for the "best place" according to the Morse interactions (3) leading locally to the minima of the quartic potential (1). Note that at equilibrium, in regular geometry each O-unit has four other O-atoms as neighbors and two other Cu-units a bit further away. In a transient tesselated pattern some O-units form rectilinear rows where the distances are smaller thus allowing lattice compressions eventually leading to soliton-like moving local excitations (Fig. 7). A special property of the two-lattice model is multistability, that is the existence of a high number of ground states instead of a single ground state in the regular lattice. Our computer simulations indicate the basic role played by the cristallographic axes formed by the O-atoms. Note that we see always patches of excited pieces of the O-axes. Since there are two axes, perpendicular to each other, the direction of the oscillations and, consequently, the lines of anisotropic liquid crystalline-like ordering, may change, so that we see in effect structures which are like tessellated patterns with patches of directional ordering. The $Cu - O$-bonds, where presumably most of the doping electrons tend to accumulate, are located right and left from the $O - O - O, \ldots$ axes. So we may imagine the existence of some "streets of local excitations" right and left besides the ordered O-axes along which added, excess electrons may travel bound to the local soliton-like excitations. Then eventually percolation paths could be established if an external electric field is also added.

In summary we may conclude that in our rather simple model we observe quite complex motions of the O-atoms oscillating in the field of the other O-atoms and in the field of the Cu-atoms. The structure mimics the effect of finite (but small) doping multistable potential landscape which is responsable for the existence of multi stable positions of the O-atoms. The field of parameters and significant parameter values is so big that we could explore so far only a small subset of all possibilities of nonlinear excitations in particular those leading to stripe-like structures. We have seen here

several types of such structures for different choices of the misfit parameter $\eta(n)$. Since the hopping transport is in zeroth approximation from copper to copper position, it remains to clarify how possible superconducting-like electronic paths are related to the above mentioned "streets of local excitations" found in our computer simulations.

Acknowledgements The authors acknowledge fruitful discussions with A. A. Alexandrov (deceased), L. Bascones, E. Brändas, L. Brizhik, A. Bussmann-Holder, L. Cruzeiro, Ch. Eilbeck, W. A. Goddard III, V. Lakhno, S. Larsson, G. Röpke, F. M. Russell, J. Tahir-Kheli and E.G. Wilson. Part of the research here reported was done when MGV was a Del Amo Visiting Scholar with the University of California at Irvine. This research was supported by the Spanish *Ministerio de Economía y Competitividad*, under Grant MAT2011-026221. A.P.C. acknowledges support from the Ministry of Education and Science of the Russian Federation under Grant 14.B37.21.0751 (2009–2013).

References

1. L. Pauling, *General Chemistry* (Dover reprint, New York, 1988)
2. T. Kihara, S. Ichimaru, *Intermolecular Forces* (Wiley, New York, 1978)
3. F.M. Russell, D.R. Collins, Phys. Lett. A **216**, 197 (1996)
4. J.L. Marín, J.C. Eilbeck, F.M. Russell, Phys. Lett. A **248**, 225 (1998)
5. J.L. Marín, F.M. Russell, J.C. Eilbeck, Phys. Lett. A **281**, 21 (2001)
6. S. Flach, K. Kladko, C.R. Willis, Phys. Rev. E **50**, 2293 (1994)
7. P.G. Kevrekidis, K.O. Rasmussen, A.R. Bishop, Phys. Rev. E **61**, 2006 (2000)
8. X. Yi, J.A.D. Wattis, H. Susanto, L.J. Cummings, J. Phys. A: Math. Theor. **42**, 355207 (2009)
9. I.A. Butt, J.A.D. Wattis, J. Phys. A: Math. Gen. **39**, 4955 (2006)
10. I.A. Butt, J.A.D. Wattis, J. Phys. A: Math. Theor. **40**, 1239 (2007)
11. Y. Yamayose, Y. Kinoshita, Y. Doi, A. Nakatani, T. Kitamura, EPL **80**, 40008 (2007)
12. K.A. Müller, Z. Phys. B: Condens. Matt. **80**, 193 (1990)
13. J. Bednorz, K.A. Müller (eds.), *Superconductivity* (Springer, Berlin, 1990)
14. A. Bussmann-Holder, A. Simon, H. Büttner, Phys. Rev. B **39**, 207 (1989)
15. A. Bussmann-Holder, A.R. Bishop, Phys. Rev. B **44**, 2853 (1991)
16. A. Bussmann-Holder, A.R. Bishop, Ferroelectrics **128**, 99 (1992)
17. D.M. Newns, C.C. Tsuei, Nat. Phys. **3**, 184 (2007)
18. R.A. Nistor, G.J. Martyna, D.M. Newns, C.C. Tsuei, M.H. Müser, Phys. Rev. B **83**, 144503 (2011)
19. A.S. Alexandrov, Phys. Scripta **83**, 038301 (2011)
20. J.M. Tranquada, B.J. Sternlieb, J.D. Axe, Y. Nakamura, S. Uchida, Nature **375**, 561 (1995)
21. V.J. Emery, S.A. Kivelson, J.M. Tranquada, PNAS **96**, 8814 (1999)
22. D. Reznik, L. Pintschovius, M. Ito, S. Likubo, M. Sato, H. Goka, M. Fujita, K. Yamada, G.D. Gu, J.M. Tranquada, Nature **440**, 1170 (2006)
23. Y. Kohsaka, C. Taylor, K. Fujita, A. Schmidt, C. Lupien, T. Hanaguri, M. Azuma, M. Takano, H. Eisaki, H. Takagi, S. Uchida, J.C. Davis, Science **315**, 1380 (2007)
24. Y. Kohsaka, C. Taylor, P. Wahl, A. Schmidt, J. Lee, K. Fujita, J.W. Alldredge, K. McElroy, J. Lee, H. Eisaki, S. Uchida, D.-H. Lee, J.C. Davis, Nature **454**, 1072 (2008)
25. K.A. Moler, Nature **468**, 643 (2010)
26. J. Zaanen, Nature **440**, 1118 (2006)
27. P.M. Morse, Phys. Rev. **34**, 57 (1929)
28. M. Rieth, *Nano-Engineering in Science and Technology* (World Scientific, Singapore, 2003)

29. M. Toda, *Theory of Nonlinear Lattices*, 2nd edn. (Springer, Berlin, 1988)
30. J. Dancz, S.A. Rice, J. Chem. Phys. **67**, 1418 (1977)
31. T.J. Rolfe, S.A. Rice, J. Dancz, J. Chem. Phys. **70**, 26 (1979)
32. A.H. Zewail, *4D Electron Microscopy: Imaging in Space and Time* (Imperial College Press, London, 2010)
33. A.P. Chetverikov, W. Ebeling, M.G. Velarde, Eur. Phys. J. B **70**, 217 (2009)
34. A.P. Chetverikov, W. Ebeling, M.G. Velarde, Physica D **240**, 1954 (2011)
35. A.P. Chetverikov, W. Ebeling, M.G. Velarde, Wave Motion **48**, 753 (2011)
36. A.P. Chetverikov, W. Ebeling, M.G. Velarde, Eur. Phys. J. B **80**, 137 (2011)
37. M.G. Velarde, W. Ebeling, A.P. Chetverikov, C. R. Mecanique **340**, 910 (2012)
38. A.P. Chetverikov, W. Ebeling, M.G. Velarde, Eur. Phys. J. B **85**, 291 (2012)
39. J. Tahir-Kheli, W.A. Goddard III, J. Phys. Chem. Lett. **2**, 2326 (2011)